Earth's Future

RESEARCH ARTICLE
10.1029/2024EF004961

The Shifting Distribution of Arctic Daily Temperatures Under Global Warming

Céline Giesse[1,2], **Dirk Notz**[1], **and Johanna Baehr**[1]

[1]Center for Earth System Research and Sustainability (CEN), Institute of Oceanography, Universität Hamburg, Hamburg, Germany, [2]Max Planck Institute for Meteorology, Hamburg, Germany

Abstract We examine daily surface air temperatures (SAT) in the Arctic under global warming, synthesizing changes in mean temperature, variability, seasonality, and extremes based on five Earth system model large ensembles from the Coupled Model Intercomparison Project Phase 6. Our analysis shows that the distribution of daily Arctic SAT changes substantially, with Arctic mean temperatures being distinguishable from pre-industrial levels on 84% and 97% of days at 1.5 and 2°C of global warming, respectively, and on virtually every day at 3°C of global warming. This shift is primarily due to the rapid rise in average temperature resulting from Arctic amplification and is exacerbated by a decrease in the variability of daily Arctic SAT of approximately 8.5% per degree of global warming. The changes in mean temperature and variability are more pronounced in the cold seasons than in summer, resulting in a weakened and shifted seasonal cycle of Arctic SAT. Moreover, the intensity and frequency of warm and cold extreme events change to varying degrees. The hottest days warm slightly more, while the coldest days warm 4–5 times more than the global average temperature, making extreme cold events rare. Changes in local SAT vary regionally across the Arctic and are most significant in areas of sea-ice loss. Our findings underscore the Arctic's amplified sensitivity to global warming and emphasize the urgent need to limit global warming to mitigate impacts on human and natural systems.

Plain Language Summary The Arctic warms about three times faster than the globe on average, impacting ecosystems and human societies profoundly. While such average warming is scientifically interesting, it is the changes in *local* temperatures on a *daily* basis that humans will be experiencing. Based on climate model simulations, we therefore examine how these daily temperatures in the Arctic change with global warming. We find that the distribution of daily Arctic temperatures shifts dramatically under global warming, barely overlapping with pre-industrial temperatures. This shift is mainly due to the amplified mean warming of the Arctic and is exacerbated by the lower fluctuations in daily temperatures with global warming. The changes in mean temperature and variability are more pronounced in winter, leading to shifting seasons and a decreasing temperature contrast between Arctic summers and winters. The intensity and frequency of warm and cold extreme events are changing. In particular, the coldest days warm 4–5 times more than the global average temperature, making extreme cold events rare. These changes vary across the Arctic, with areas losing sea ice experiencing the most significant shifts. This study emphasizes the urgent need to reduce global warming to protect Arctic ecosystems and communities.

Key Points:

- The distribution of daily Arctic temperatures shifts drastically under global warming, barely overlapping with pre-industrial temperatures
- This is due to amplified Arctic warming, along with a reduction in the variability of daily temperatures
- The hottest days warm slightly more, while the coldest days warm 4–5 times more than the global mean temperature

Supporting Information:

Supporting Information may be found in the online version of this article.

Correspondence to:

C. Giesse,
celine.giesse@uni-hamburg.de

Citation:

Giesse, C., Notz, D., & Baehr, J. (2024). The shifting distribution of Arctic daily temperatures under global warming. *Earth's Future*, *12*, e2024EF004961. https://doi.org/10.1029/2024EF004961

Received 30 MAY 2024
Accepted 7 OCT 2024

Author Contributions:

Conceptualization: Céline Giesse, Dirk Notz, Johanna Baehr
Formal analysis: Céline Giesse
Funding acquisition: Johanna Baehr
Investigation: Céline Giesse
Methodology: Céline Giesse
Project administration: Céline Giesse
Supervision: Dirk Notz, Johanna Baehr
Visualization: Céline Giesse
Writing – original draft: Céline Giesse
Writing – review & editing: Céline Giesse, Dirk Notz

1. Introduction

The Arctic is warming faster than any other region in the world and is transitioning to a new Arctic climate state (Landrum & Holland, 2020). With the detectable emergence of Arctic amplification in the last century (England et al., 2021), surface temperatures in the Arctic have warmed more than twice as fast as in the global average (Serreze & Barry, 2011). In recent decades, the Arctic has even warmed almost four times faster than the global average (Chylek et al., 2022; Rantanen et al., 2022). However, recent studies have shown that the externally forced Arctic amplification has consistently remained close to three, with the recent very high value of Arctic amplification attributed to an amplifying effect of natural variability (Sweeney et al., 2023; Zhou et al., 2024). The Arctic amplification is caused by an interplay of different processes and feedback mechanisms, most importantly temperature and surface-albedo feedbacks (Pithan & Mauritsen, 2014; Previdi et al., 2021; Wendisch et al., 2023). It has profound impacts on human and natural systems within and outside the Arctic (AMAP, 2021; Jeffries et al., 2013; Previdi et al., 2021), including rapid loss of sea ice, melting of the Greenland ice sheet, thawing of

permafrost, coastal erosion, wildfires, threats to terrestrial and marine ecosystems, and the risk of crossing multiple climate tipping points (Armstrong McKay et al., 2022).

Some of the most severe impacts of climate change on ecosystems and human society are caused by extreme events rather than changes in climatic means (e.g., Walsh et al., 2020). To understand and prepare for climate change in the Arctic, it is therefore crucial to know not only how Arctic average temperatures evolve under global warming, but also how the distribution of local, daily temperatures within the region is changing. The rapid pace of Arctic climate change is reflected not only in the highest mean warming rates on Earth but also in a reduced and shifted seasonal temperature cycle (Chen et al., 2019; Dwyer et al., 2012; Polyakov et al., 2024), decreasing temperature variability (Bathiany et al., 2018; Borodina et al., 2017; Chen et al., 2019; Dai & Deng, 2021; Holmes et al., 2016; Olonscheck et al., 2021; Ylhäisi & Räisänen, 2014), and an increasing number of extreme temperature events (Seneviratne et al., 2021; Walsh et al., 2020), such as summer heat waves in the terrestrial Arctic (Dobricic et al., 2020) and winter warming events over the Arctic Ocean (Graham et al., 2017; Moore, 2016). While individual aspects of the Arctic temperature evolution under global warming have been studied before (often in the context of global studies), a synthesis that considers changes in the entire temperature distribution within a common framework is lacking.

In light of this importance of changes in the statistics of daily surface air temperatures (SAT), we here assess their changes in the Arctic for a given level of global warming, synthesizing and putting into perspective changes in Arctic mean temperature, variability, seasonality, and extremes. In contrast to many previous studies, we analyze the Arctic SAT response in the framework of global warming levels (GWLs), providing results that are largely independent of time and warming scenario and of high interest for policy-making (IPCC, 2021). Moreover, we provide a detailed picture of the regional differences in Arctic temperature changes under global warming that is not available from global studies. We base our analysis on five single-model initial-condition large ensembles (SMILEs; Deser et al., 2020) from the sixth phase of the Coupled Model Intercomparison Project (CMIP6; Eyring et al., 2016). Each of the SMILEs contains 40–50 ensemble members that simulate the climate under identical external forcing and model configurations but with slightly perturbed initial conditions, allowing us to derive robust estimates of internal temperature variability and extremes (Deser et al., 2020; Olonscheck et al., 2021). The data and analysis methods are described in Section 2, followed by the assessment of Arctic SAT at different levels of global warming, divided into changes in the temperature distribution (Section 3), the seasonal temperature cycle (Section 4) and extreme temperatures (Section 5), and our conclusions (Section 6).

2. Data and Methods

2.1. Large Ensemble Simulations

We analyze data from five SMILEs from the latest CMIP6 (Eyring et al., 2016) generation of climate models that provide at least 40 ensemble members, namely: MPI-ESM1.2-LR (50 members; Olonscheck et al., 2023), CanESM5 (50 members; Swart et al., 2019), MIROC6 (50 members; Tatebe et al., 2019), ACCESS-ESM1.5 (40 members; Ziehn et al., 2020), and EC-Earth3 (50 members; Wyser et al., 2021). We combine historical simulations (years 1850–2014; for EC-Earth3 data is available only starting from year 1970) and future projections (years 2015–2100) from the high-emission SSP5-8.5 scenario. To test for pathway dependence, we additionally use MPI-ESM1.2-LR simulations under the SSP1-2.6 scenario. For an overview of the model simulations used in this study, see also Table S1 in Supporting Information S1.

From these simulations, we compute the annual-mean global-mean surface air temperature (GSAT) and analyze the corresponding daily SAT in the Arctic domain, defined here as north of 66°N. Temperature anomalies are computed with respect to the pre-industrial period from 1850 to 1900 (consistent with IPCC (2021)). The later initial year in the EC-Earth3 model is taken care of by computing anomalies with respect to the period 1970–2000 and adding the difference between the periods 1970–2000 and 1850–1900 from the MPI-ESM simulations. We further use monthly sea-ice concentration data from the simulations to show seasonal average sea-ice edges, defined as the 15%-contour line of sea-ice concentration, in the spatial figures.

Note that CMIP6 models have some common biases in simulating the Arctic climate. Comparison with atmospheric reanalyses shows that CMIP6 models commonly simulate overly cold Arctic winter SAT related to overestimated sea-ice extents and overly high inter-annual variability of Arctic winter SAT (Cai et al., 2021; Davy & Outten, 2020). However, a recent study shows that the cool Arctic surface temperatures simulated by climate

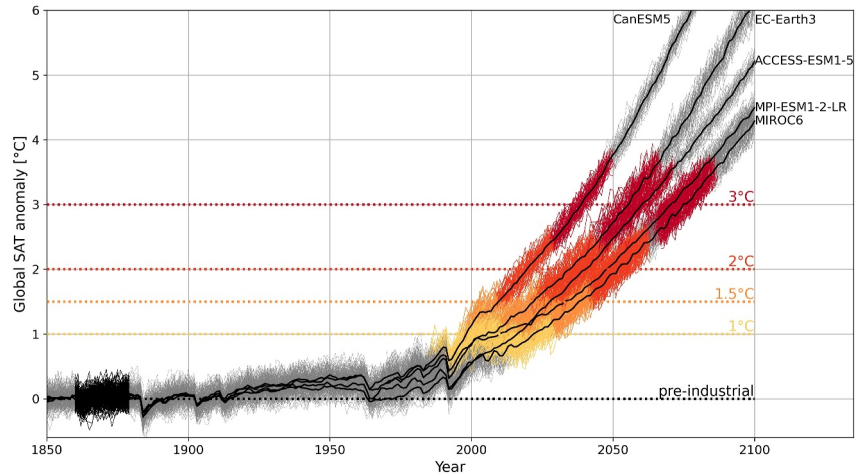

Figure 1. Sampling of global warming levels. Time-series of annual global-mean SAT anomaly of each ensemble member (thin gray lines) and the ensemble mean (black lines) of the five considered SMILEs. The colored parts of the lines mark the data that is selected for the different GWLs (pre-industrial: black, 1°C GWL: yellow, 1.5°C GWL: light orange, 2°C GWL: dark orange, 3°C GWL: red).

models are closer to satellite-based data than the ERA5 reanalysis (Tian et al., 2024), re-strengthening the confidence in the model results. There is a considerable inter-model spread in how well CMIP6 models capture Arctic SAT and its tempo-spatial variability, with the MPI-ESM-LR model used here being among the best-performing models (Cai et al., 2021). Additionally, there is a chance that important processes are missing from the models. For example, there is a risk of abrupt climate change triggered by the crossing of thresholds in the climate system (Alley et al., 2003; Duarte et al., 2012), which some argue is already occurring in the Arctic (Jansen et al., 2020). This could potentially alter the Arctic climate response to global warming in ways not predicted by climate models. Nevertheless, these models are currently the best tools available to assess changes in the statistical distribution of SAT which is why we use them for the purpose of this study.

2.2. Global Warming Levels

We analyze Arctic SAT at specific global warming levels (GWLs) by selecting representative data samples for the climate at pre-industrial levels, 1, 1.5, 2, and 3°C of global warming using a time sampling approach (James et al., 2017) (colored lines in Figure 1). The resulting data samples contain 800 or 1,000 simulations years (depending on the model ensemble size) per model and GWL, allowing for a robust analysis of variability and extremes. We follow the methodology used by the IPCC (IPCC, 2021; Seneviratne et al., 2021): For each individual ensemble member, we identify the year in which the 20-year rolling average GSAT anomaly first reaches the given GWL and include the 20-year period around this year into the data sample. Due to internal variability, the timing of the considered 20-year periods can differ between ensemble members, but their average GSAT anomaly always corresponds to the target GWL. For the pre-industrial conditions, we simply take the 20-year period 1860–1879 for all ensemble members of all models. The GWL samples based on SSP5-8.5 simulations represent a transient climate state and are therefore subject to a warming trend. We remove the warming trend from the GWL samples by subtracting the linear trend of the ensemble-mean 20-year SAT time series at each day of the year (DOY) and grid cell from each ensemble member. In order to test whether the results differ between a transient and near-equilibrium climate state, we additionally compare the 20-year period 2055–2074 with a stable GSAT anomaly of 1.6°C from the SSP1-2.6 simulations to a transient sample with the same average GSAT anomaly from the SSP5-8.5 simulations in MPI-ESM.

In addition to the GWL approach, for some parts of the analysis we directly evaluate Arctic SAT against the corresponding ensemble-mean GSAT anomaly (black lines in Figure 1) in each simulation year. With this approach, the data sample used to compute statistical properties, such as mean or variability, is reduced to the model ensemble size, making it less robust and not suitable for analyzing extremes. However, this approach provides us with a continuous time series and allows us to analyze whether Arctic SAT and its statistical properties respond linearly to global warming. If so, we compute the rates of change with global warming as the

regression coefficient of a linear ordinary least squares regression. To avoid over-representation of the historical period with low global warming levels and to ensure comparison of identical ranges of global warming across climate models, we restrict the linear regression to data points within the range of 0.5–4°C of global warming.

2.3. Analysis of Arctic Temperatures Under Global Warming

We divide the analysis of changes in Arctic SAT under global warming into three parts: changes in the temperature distribution, the seasonal temperature cycle, and extreme temperatures.

In Section 3, we analyze the probability distribution of daily SAT in the Arctic for the different GWLs in different seasons and for the entire year. To remove temperature variations resulting only from the seasonal cycle, we deseasonalize the data beforehand. To quantify the distinguishability of the probability distribution at a certain GWL from the pre-industrial distribution, we calculate the percentage of days that are warmer than the 95th percentile of the pre-industrial distribution. This gives us the proportion of days that are warmer under global warming than the extremely warm days at pre-industrial conditions at the same time of the year (i.e., without the seasonal cycle). From the probability distribution, we further compute the mean temperature and variability of daily temperatures within a given season. The variability of daily temperatures is computed as the standard deviation of daily, deseasonalized SAT across all days within the considered season of all ensemble members and years of the GWL sample. Computing the variability across ensemble members is equivalent to computing the variability across years in time, following the quasi-ergodic assumption (Hingray & Säid, 2014; Olonscheck & Notz, 2017). Note that the variability of daily temperatures includes both variations within a single year or season (sub-seasonal variability) and variations between individual years (inter-annual variability). Where we show Arctic-mean SAT variability, we compute the variability as the spatial average of the local temperature variability computed at grid-cell level. Note that this is different from the variability of spatially averaged temperature, which is considerably smaller as local variability is suppressed by averaging over the spatially correlated temperature field.

In Section 4, we analyze the seasonal cycle of Arctic SAT. We compute the seasonal cycle for a given GWL as the average SAT on each DOY, either at grid-cell level for the local seasonal cycle or for the Arctic mean. The amplitude is defined as the difference between the annual maximum and minimum temperatures of the seasonal cycle. The phase of the seasonal cycle is described by the average DOY of the annual minimum/maximum SAT over the GWL sample.

In Section 5, we use a block maxima/minima approach to study warm/cold temperature extremes. For this, we take the temperature of the hottest/coldest day, given by the annual maximum/minimum daily mean SAT (T_{max}/T_{min}), in each simulation year and ensemble member at each grid cell. Based on the GWL samples, we compute empirical return levels of warm and cold extreme temperatures on grid-cell level. The large sample sizes (n = 800–1,000) allow us to determine return levels empirically, even for high return periods, without the need to parameterize the tails of the distribution with extreme value statistics. For the Arctic-mean return levels, we compute the spatial average of the local return levels (in contrast to computing return levels of extreme Arctic-mean temperatures). From the return levels, we further compute changes in the intensity and frequency of extreme temperatures relative to the pre-industrial period. As the EC-Earth3 data only starts in 1970, this model is missing in the multi-model comparison.

3. Changing Distribution of Daily Temperatures

The probability distribution of daily Arctic-mean SAT after removal of the seasonal cycle (see Section 2.3) changes considerably with global warming, as shown for the different seasons in Figure 2a, exemplarily based on the MPI-ESM. The overlap between the temperature distributions under pre-industrial conditions and the global warming targets of the Paris Agreement is small, that is, daily temperatures are distinguishable from pre-industrial levels (Figure 2b). Considering the year-round temperature distributions, at 1°C GWL about 50% [cross-model range: 15%…74%] of the days are warmer than extremely warm days at the same time of year under pre-industrial conditions. At 1.5 and 2°C GWL the proportion rises to 84% [61%…95%] and 97% [93%…100%], respectively. At 3°C GWL, the models agree that virtually all days will be hotter than the extreme warm days at pre-industrial levels. This illustrates the transition to a new Arctic climate state, in which Arctic-mean temperatures that were previously considered extremely warm at a given time of year will represent a cold extreme or no longer occur at all. While this general finding holds across all seasons, the degree of overlap differs. This is due to the seasonality

10.1029/2024EF004961

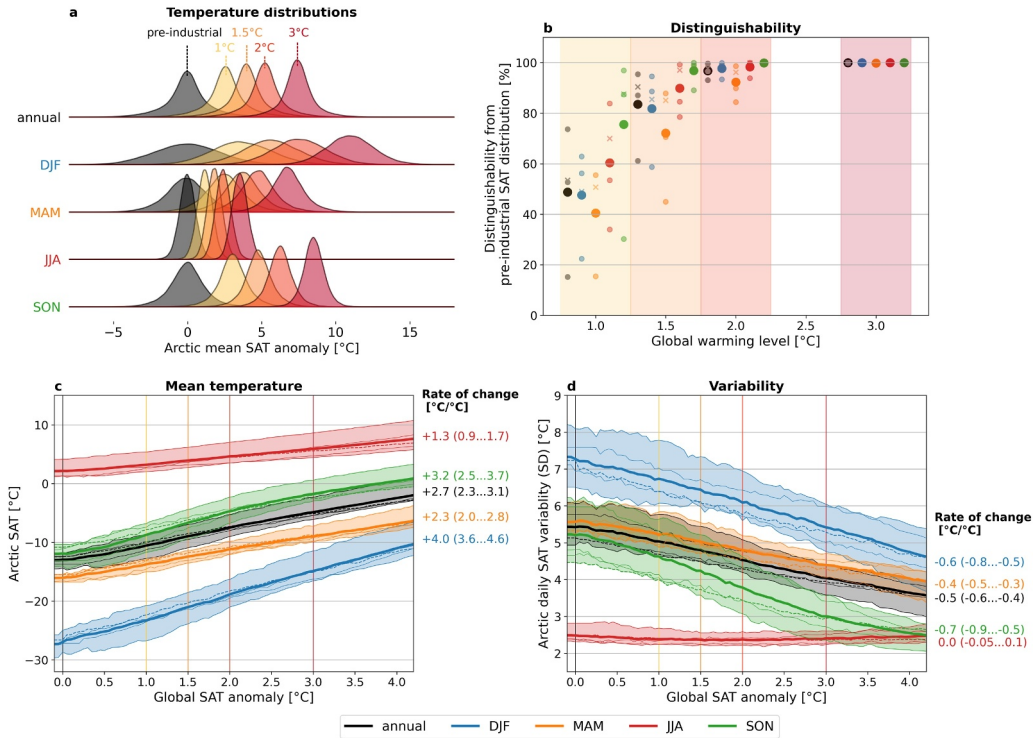

Figure 2. Arctic mean changes in the distribution of daily SAT. (a) Probability distributions of the deseasonalized daily Arctic-mean SAT for the whole year and each season for different GWLs in the MPI-ESM. (b) Distinguishability of the probability distributions at different GWLs with the pre-industrial distribution in all considered models, based on the percentage of days that are warmer than the 95th percentile of the pre-industrial distribution. Large dots show the multi-model mean, small dots show the individual models and crosses indicate MPI-ESM. (c, d) Arctic-mean annual and seasonal mean (c) and variability (d) of deseasonalized daily SAT in all models as a function of global warming. The thick lines show the multi-model mean, the thin lines show the individual models with the dashed line indicating MPI-ESM, and the shading illustrates the multi-model range. The rates of change with global warming based on linear regression are given for the multi-model average, with the range of the individual models in parentheses.

of the Arctic amplification and the seasonality of the temperature variability. In autumn, when a large mean warming and relatively low temperature variability coincide, the temperature distributions for different GWLs are particularly distinguishable.

The major change of the temperature distribution is caused by the shift in mean temperature rather than by a changing distribution of temperatures around this mean. The Arctic-mean SAT increases approximately linearly with global warming (Figure 2c). The Arctic amplification, computed as the linear trends of Arctic versus global SAT anomalies, underlies a strong seasonality (Figure 2c and Figure S1 in Supporting Information S1). The models simulate an annual Arctic amplification of 2.7 [2.3…3.1]°C per degree of global warming, with the largest seasonal mean warming in winter (4.0 [3.6…4.6]°C/°C), followed by autumn (3.2 [2.5…3.7]°C/°C), spring (2.3 [2.0…2.8]°C/°C), and summer (1.3 [0.9…1.7]°C/°C). This seasonal asymmetry in Arctic warming is closely linked to sea-ice loss (Bintanja & Van Der Linden, 2013; Dai et al., 2019; Previdi et al., 2021; Screen & Simmonds, 2010), amplifying the intraseasonal storage and release of heat (Chung et al., 2021; Hahn et al., 2022) as well as the positive lapse-rate feedback in winter (Boeke et al., 2021; Feldl et al., 2020). The estimated magnitude of Arctic amplification is in good agreement with other model-based estimates reported in the literature (Chylek et al., 2022; Holland & Landrum, 2021; Rantanen et al., 2022) and with the estimate of externally forced Arctic amplification in the historical period of about three (Zhou et al., 2024). Note that the assumed linearity is only an approximation and that the rate of Arctic warming decreases for higher levels of global warming, particularly in autumn. This flattening is caused by a weakened ice-albedo feedback due to the loss of sea ice (Holland & Landrum, 2021; Ono et al., 2022), which is fastest around the sea-ice minimum in September. The considered models project the Arctic to become practically sea-ice-free (i.e., the sea-ice area is less than 1 million km^2) in

September between 1.9 and 2.9°C of global warming based on their ensemble mean (Figure S2 in Supporting Information S1).

While mean temperature increases, the variability of Arctic daily temperatures decreases in all seasons except summer, consistently throughout the models (Figure 2d) and in accordance with previous model-based studies (Chen et al., 2019; Dai & Deng, 2021; Ylhäisi & Räisänen, 2014). The Arctic mean of the year-round local temperature variability decreases by −0.5 [−0.6…−0.4]°C in standard deviation per degree of global warming, which corresponds to 8.5 [7.2…10.4]% of its pre-industrial value. Seasonally, the decrease in variability is strongest in autumn (−0.7 [−0.9…−0.5]°C/°C), followed by winter (−0.6 [−0.8…0.5]°C/°C) and spring (−0.4 [−0.5…−0.3]°C/°C). While annually, in winter, and in spring, the variability decreases approximately linearly in the considered global warming range, in autumn, the decrease flattens with increasing GWL as the seasonal sea ice is lost completely. At 4°C of global warming, the Arctic-mean SAT variability in autumn has approximately halved. In contrast to the other seasons, the Arctic mean of summer SAT variability stays close to constant in all models. The consistent negative trend in the variability of Arctic daily SAT in climate models is less evident from atmospheric reanalyses (Chen et al., 2019; Davy & Outten, 2020), which show positive trends over the central Arctic in March (Davy & Outten, 2020). The reason is, however, not clear and could be due to natural variability, poorly represented surface coupling processes in the climate models, or inaccuracies of the reanalysis (Davy & Outten, 2020; Tian et al., 2024).

Spatially, the warming of the Arctic and the changes in variability are not uniform. The models consistently show the strongest changes in SAT distribution over areas of sea-ice loss, as shown exemplarily for the MPI-ESM (Figure 3). This concerns, in particular, the northern Barents Sea, where local winter temperatures warm by up to 17.5°C at 2°C of global warming (in MPI-ESM, Figure 3d). This hotspot of warming is also evident from observations (Isaksen et al., 2022) and mainly caused by the loss of cold-season sea ice in that area and the resulting "Atlantification" of the northern Barents Sea (Ingvaldsen et al., 2021; Lind et al., 2018; Polyakov et al., 2017). At the same time, SAT variability in the northern Barents Sea reduces drastically. In winter, the local variability reduces by up to 6.4°C in standard deviation at 2°C GWL (Figure 3e), corresponding to two-thirds of the pre-industrial value. As a result, the local SAT distribution in the northern Barents Sea not only shifts but changes its shape substantially, especially in winter (Figure 3f) but also in the other cold seasons. In autumn, the enhanced warming and strong reduction in variability is not restricted to the Atlantic sector but occurs around the entire edge of the Arctic Ocean, where sea ice is lost seasonally, particularly in the Chukchi Sea, located at the connection to the Pacific (Figures 3m and 3n). The rest of the Arctic (central Arctic, North Atlantic sector, and land areas including the Greenland ice sheet) also experiences warming and decreasing annual and cold season temperature variability, with the weakest changes over the open waters of the northern North Atlantic and over Greenland. The decrease in temperature variability is caused primarily by the retreat of sea ice, which reduces the insulation between ocean and atmosphere and increases the effective heat capacity of the ocean (Borodina et al., 2017; Huntingford et al., 2013; Olonscheck et al., 2021; Stouffer & Wetherald, 2007). In addition, reduced thermal advection due to a weakened meridional temperature gradient resulting from Arctic amplification further reduces temperature variability extending into the northern mid-latitudes (Blackport et al., 2021; Collow et al., 2019; Dai & Deng, 2021; Holmes et al., 2016; Schneider et al., 2015; Screen, 2014; Tamarin-Brodsky et al., 2020).

In summer, on the contrary, there is practically no warming over the central Arctic Ocean, as the sea-ice cover keeps the SAT at freezing temperature (Borodina et al., 2017) and excess heat goes into melting the sea ice. The SAT over surrounding open waters and land areas, however, warms at rates comparable to the other seasons. As the SAT over ice-covered areas stays at freezing temperatures, SAT variability in the central Arctic in summer is small at any level of global warming. While the SAT variability slightly decreases over the North Atlantic and Greenland, it slightly increases over land areas and ocean areas that transition from ice-covered to seasonally ice-free, such as the northern Barents and Kara Sea. The net effect of positive and negative changes in variability is negligible in the Arctic spatial average.

Note that the variability of daily temperatures shown here includes both temperature variations within a season (sub-seasonal variability) and variations between the seasonal mean temperature in different years (inter-annual variability). A decomposition into these components reveals that the dominant sub-seasonal variability consistently decreases in the entire Arctic (except in summer), whereas the inter-annual variability locally increases in areas around the new sea-ice edge (in all seasons) as the sea-ice extent varies from year to year (not shown).

10.1029/2024EF004961

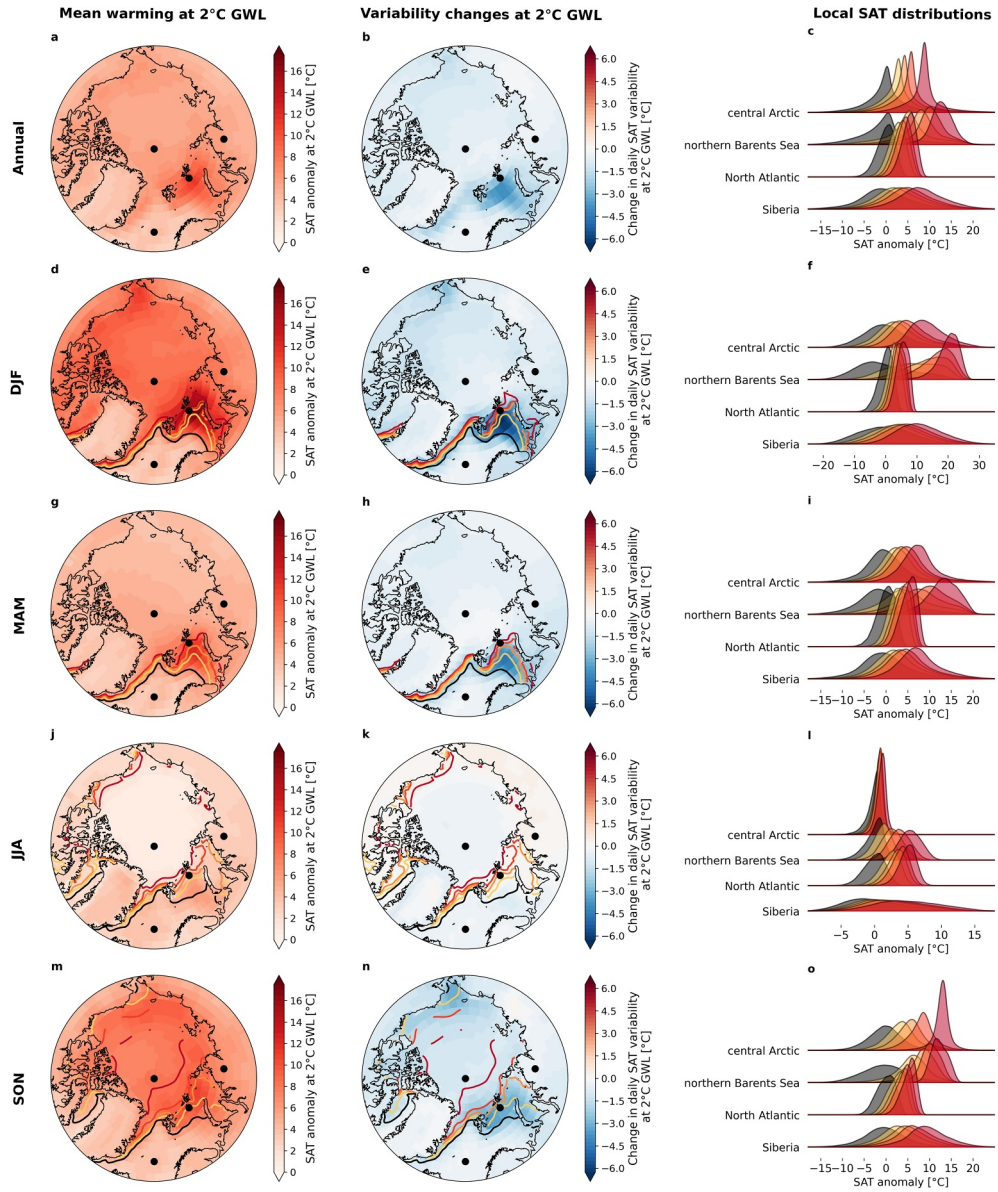

Figure 3. Local changes in the distribution of daily SAT in the Arctic. Changes in annual and seasonal mean SAT (left column) and variability of local daily SAT (middle column) at 2°C GWL with respect to pre-industrial conditions in MPI-ESM. The colored lines show the seasonal sea sea-ice edges at different GWLs. Right column: Probability distribution of the local deseasonalized daily SAT in MPI-ESM for different GWLs at four selected locations (marked as dots on the maps), representing the central Arctic (90°N, 0°E), northern Barents Sea (79°N, 50°E), North Atlantic (70°N, 0°E), and Siberia (73°N, 98°E).

Note further that the analysis is based on projections under the high-emission scenario SSP5-8.5, that is, for a rapidly warming climate. The climate response to global warming can depend on the emission pathway (James et al., 2017) and differ between transient and equilibrium climate states (King et al., 2020, 2021). Repeating the analysis based on MPI-ESM SSP1-2.6 scenario simulations (Figure S3a in Supporting Information S1), we find some differences in the spatial patterns of mean SAT and variability of daily SAT in a transient and near-equilibrium climate state with the same level of global warming (Figure S4 in Supporting Information S1). For instance, SAT over land and sea-ice covered areas is higher in a transient climate (except in spring) as it responds faster than SAT over the open ocean (King et al., 2020). The magnitude of the differences in local SAT between the transient and the near-equilibrium states is, however, small compared to the locally forced warming, and positive and negative differences partially cancel out in the spatial average. As a result, the response of Arctic-

10.1029/2024EF004961

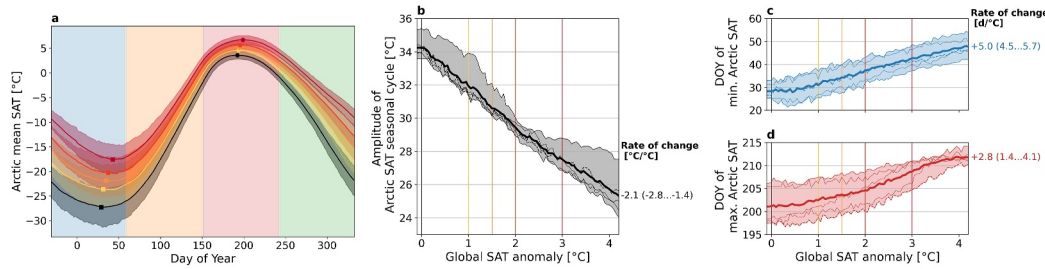

Figure 4. Arctic mean changes in the seasonal cycle of SAT. (a) Seasonal cycle of Arctic-mean SAT at different GWLs in MPI-ESM. The shading shows the 90% confidence interval based on individual year's SAT cycle. The circles/squares mark the average DOY of minimum/maximum daily mean SAT. (b–d) Arctic mean of the amplitude (b), DOY of minimum temperature (c), and DOY of maximum temperature (d) of the local seasonal cycle in all models as a function of global warming. The thick lines show the multi-model mean, the thin lines show the individual models with the dashed line indicating MPI-ESM, and the shading illustrates the multi-model range. The rates of change with global warming based on linear regression are given for the multi-model average, with the range of the individual models in parentheses.

mean SAT to global warming is largely independent of the underlying scenario (Figure S3b in Supporting Information S1). The only exception is the response of annual, summer, and autumn Arctic SAT variability, which shows a remarkable pathway dependence, with variability increasing significantly again after external greenhouse gas forcing ceases and the global mean temperature stabilizes (Figure S3c in Supporting Information S1). The reasons for this finding, which indicates some limitation of our transient GWL approach for a robust analysis of temperature variability, are currently unclear and require further investigation.

4. Changing Seasonal Temperature Cycle

Since the Arctic amplification acts strongest in early winter and weakest in summer (see above and Figure S1 in Supporting Information S1), it alters the seasonal cycle of SAT in the Arctic. As known from previous studies (Chen et al., 2019; Dwyer et al., 2012; Mann & Park, 1996; Polyakov et al., 2024; Stine et al., 2009; Thomson, 1995) and visible from the seasonal cycle of Arctic-mean SAT at the different GWLs (Figure 4a), the amplitude is decreased and the phase is delayed with global warming. The amplitude of the seasonal cycle decreases approximately linearly at a rate of −2.1 [−2.8…−1.4]°C, corresponding to about 6.2% of its pre-industrial value, per degree of global warming (Figure 4b). In addition to the reduced internal variability, the reduced seasonal temperature contrast further diminishes the range of temperatures experienced in the Arctic throughout the year. Moreover, the DOY of minimum Arctic SAT is delayed by 5 [4.5…5.7] days and the DOY of maximum Arctic SAT is delayed by 2.8 [1.4…4.1] days per degree of global warming (Figures 4c and 4d). This implies a shift in the seasons, with the coldest days shifting from the end of January under pre-industrial conditions to mid-February at 4°C of global warming and the warmest days shifting toward the end of July. While the minimum temperature shifts linearly with global warming, the shift in maximum temperature saturates at about 4°C of global warming as the summer sea ice is lost completely. The modulation of the seasonal cycle of Arctic SAT is also evident from reanalysis data of the recent past, which show an even larger reduction in the seasonal cycle amplitude of 2°C from 1979 to 2021 (Polyakov et al., 2024), a period of particularly strong Arctic amplification (Rantanen et al., 2022).

Spatially, the amplitude of the local SAT cycle (Figure 5a for MPI-ESM) decreases most where strong winter warming and weak summer warming coincide. This is especially the case in the northern Barents Sea region, where the amplitude decreases by up to 12°C at 2°C of global warming and the formerly pronounced seasonal cycle transitions to a seasonally almost uniform SAT (Figure 5e), similar to that of the North Atlantic sector (Figure 5f). The amplitude of the seasonal cycle of SAT also decreases substantially in the central Arctic (−7.3°C at 2°C GWL) and slightly less (−4°C at 2°C GWL) in the terrestrial Arctic. In contrast, the amplitude remains constant over the North Atlantic sector due to seasonally constant warming and even increases over Greenland, where summer warming exceeds winter warming.

The pattern of the shift in the day of minimum temperature (Figure 5b) resembles the change in amplitude. The annual minimum temperature occurs later in the year in most of the Arctic, with the strongest shift in the northern Barents Sea (up to 29 days at 2°C GWL), followed by the central Arctic Ocean and the terrestrial Arctic. Over the

10.1029/2024EF004961

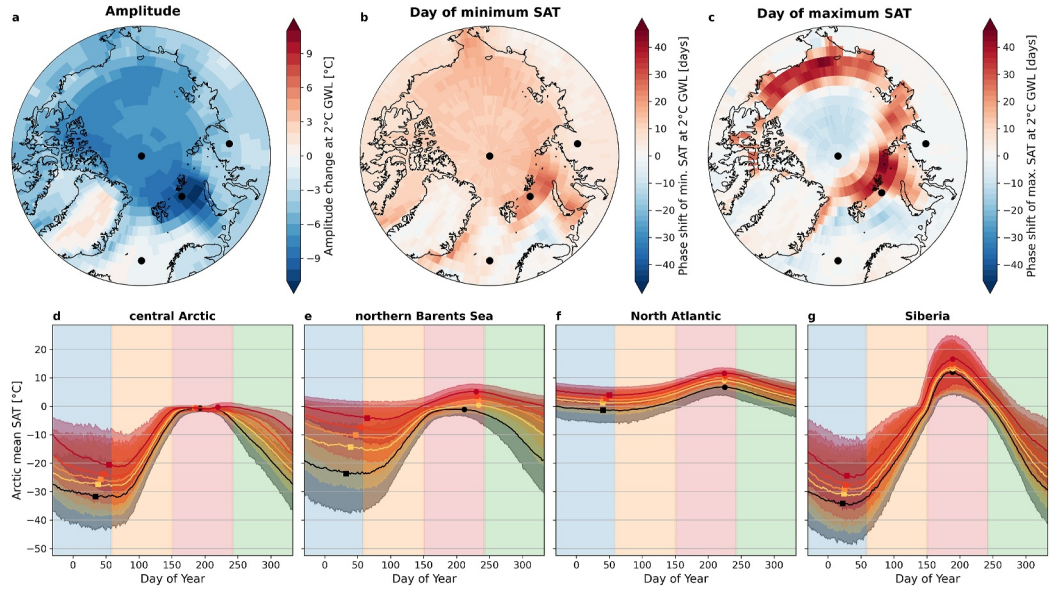

Figure 5. Local changes in the seasonal cycle of SAT in the Arctic. Changes in the amplitude (a), DOY of minimum temperature (b), and DOY of maximum temperature (c) of the seasonal cycle at 2°C GWL with respect to pre-industrial conditions in MPI-ESM. (d–g) Local seasonal cycle of SAT in MPI-ESM for different GWLs at four selected locations (marked as dots on the maps), representing the central Arctic (90°N, 0°E), northern Barents Sea (79°N, 50°E), North Atlantic (70°N, 0°E), and Siberia (73°N, 98°E). The shading shows the 90% confidence interval based on individual year's SAT cycle. The circles/squares mark the average day of minimum/maximum daily mean SAT.

North Atlantic and Greenland, there is no significant shift in the day of minimum temperature. The delay in the coldest days results from the seasonality of Arctic warming, which is higher in early winter than in late winter (Figure S1 in Supporting Information S1). Since the seasonal peak of Arctic warming shifts to later days of the year with increasing CO_2-forcing as shown by Liang et al. (2022), we would expect the phase delay in the day of minimum SAT to cease at even higher global warming rates than considered here.

The shift in the day of maximum temperature, on the other hand, is much more localized, confined to areas of summer sea-ice loss. In these areas, the ocean takes up additional heat during the summer season and delays the cooling of the overlying air by up to 46 days at 2°C GWL. In the remaining Arctic, the shift in the day of maximum temperature is small or even directed toward earlier days. The localized nature of the delay in the warmest days is less obvious from studies looking at the global scale (Chen et al., 2019).

5. Changing Temperature Extremes

The mean warming and the changes in variability alter the intensity and frequency of extreme SAT in the Arctic. Based on the Arctic-mean empirical return levels of annual maximum and minimum SAT (Figures 6a and 6d), we compute the changes in intensity (Figures 6b and 6e) and frequency (Figures 6c and 6f) of Arctic warm and cold extreme temperatures with respect to pre-industrial conditions.

The intensity of extreme temperatures changes approximately linearly with global warming, as found for various regions in previous studies (Seneviratne et al., 2016; Wartenburger et al., 2017). The intensity changes are slightly larger for higher return periods but are not very sensitive to the return period. The temperature of the hottest days in the Arctic increases slightly (about 1.3 times) more than the global mean temperature. For example, at 2°C of global warming, the models project an intensity increase of 2.5 [2.2…3.1]°C for a 10-year warm extreme event and of 2.7 [2.3…3.3]°C for a 100-year warm extreme event (Figure 6b). As winter temperatures rise faster than summer temperatures, the intensity of cold extreme events decreases more than the intensity of warm extremes increases. The temperature of the coldest days warm about 4–5 times more than the global average temperature. For example, at 2°C of global warming, a 10-year cold extreme event is 9.0 [7.6…10.0]°C and a 100-year cold extreme event is 9.2° [7.8…10.1]°C warmer than under pre-industrial conditions (Figure 6e). While the stronger increase in annual minimum than in annual maximum temperatures can be observed globally, the warming of the

10.1029/2024EF004961

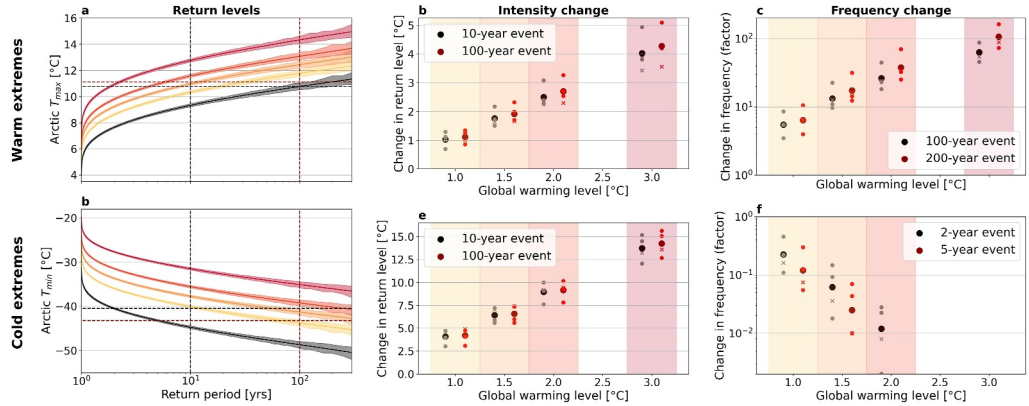

Figure 6. Arctic-mean changes in extreme SAT. (a, d) Arctic-mean return levels of warm and cold extremes (defined as annual maximum and minimum daily SAT) in MPI-ESM. The shading shows the uncertainty range of the return levels, estimated as the 90% confidence intervals based on bootstrap-resampling with replacement with 1,000 repetitions. (b, e) Intensity change with respect to pre-industrial conditions of 10- and 100-year warm and cold extreme events for different global warming levels. (c, f) Frequency change (as factor) of warm extremes with return periods of 100 and 200 years under pre-industrial conditions and cold extremes with return periods of 2 and 5 years under pre-industrial conditions for different global warming levels. The large dots show the multi-model mean, the small dots show the individual models with the crosses indicating MPI-ESM.

coldest days is particularly high in the Arctic region (Seneviratne et al., 2021). The dampened seasonal cycle of Arctic SAT (Section 4) contributes decisively to the faster rate of change of winter cold extremes than that of summer warm extremes (Polyakov et al., 2024).

Unlike intensity, frequency changes nonlinearly, almost exponentially, with global warming, as has been found for temperature extremes in other regions (Fischer & Knutti, 2015; Kharin et al., 2018). In addition, the changes in frequency are very sensitive to the return level considered and vary widely between models, especially for the cold extremes, leading to considerable uncertainties. For example, a warm extreme event with a return period of 100 years under pre-industrial conditions, occurs 13 [10…23] times more frequently at 1.5°C GWL (i.e., every 8 years), 26 [18…45] times more frequently at 2°C GWL (i.e., every 4 years), and 63 [46…88] times more frequently at 3°C GWL (i.e., in more than half of the years). A warm extreme event with a return period of 200 years under pre-industrial conditions, occurs 17 [12…32] times more frequently at 1.5°C GWL (i.e., every 12 years), 37 [25…70] times more frequently at 2°C GWL (i.e., every 5 years), and 106 [73…163] times more frequently at 3°C GWL (i.e., about every second year). The frequency of cold extreme events changes even more drastically. For example, a cold extreme with a return period of 2 years under pre-industrial conditions occurs on average every 32 [14…112] years at 1.5°C GWL, every 166 [72…1,000] years at 2°C GWL, and less than once in 1,000 years at 3°C GWL. A cold extreme event with a return period of 5 years under pre-industrial conditions occurs on average every 200 [115…505] years at 1.5°C GWL and less than once in 1,000 years at 2°C of global warming.

Spatially, the warming of the hottest and coldest daily temperatures (Figures 7a and 7c) resemble the pattern of summer and winter mean warming, especially for warm extremes, as changes in the internal variability of summer SAT are small. The intensity of warm extreme events (Figure 7a) increases most in areas of sea-ice loss such as the northern Barents Sea but also over central Greenland and the terrestrial Arctic. In the central Arctic, however, the intensity of warm extreme events remains virtually unchanged as long as summer sea ice is present, keeping the overlying air at freezing temperatures. This is also evident from the return levels for different GWLs in the central Arctic (Figure 7e), where at up to 2°C of global warming the return levels remain flat around 0°C and only at 3°C GWL the return levels start to increase with the return period and the curve takes the shape expected from a generalized extreme value distribution.

Due to the decreasing internal variability in winter, the coldest days warm even more than average winter temperatures, leading to substantial decreases in cold extreme event intensity (Figure 7c). Most pronounced in the Barents Sea, cold extreme events with a return period of 10 years are up to 29.6°C warmer at 2°C of global

10.1029/2024EF004961

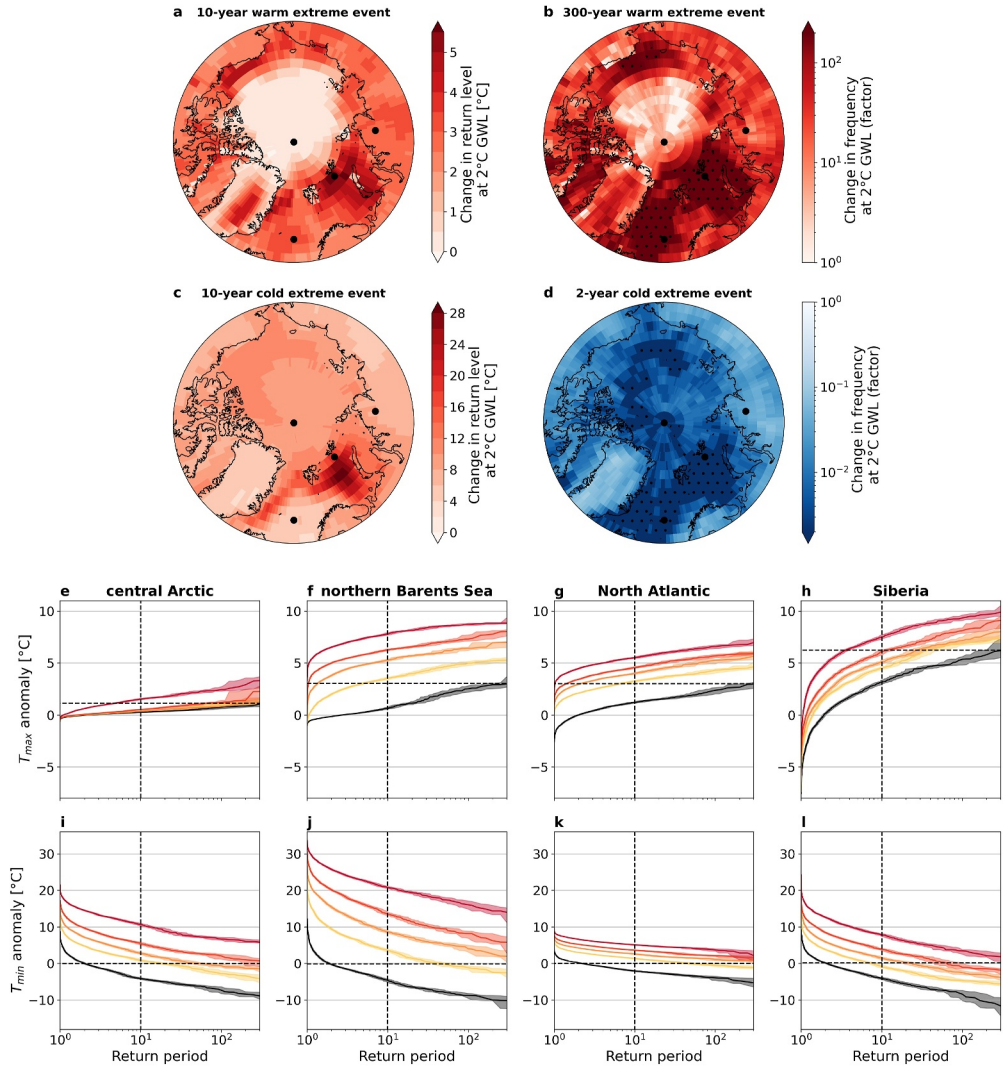

Figure 7. Local changes in extreme SAT. (a–d) Local changes in intensity of (a) warm extremes (10-year event) and (c) cold extremes (10-year event) and in frequency of (b) warm extremes (200-year event at pre-industrial levels) and (d) cold extremes (2-year event at pre-industrial levels) at 2°C GWL with respect to pre-industrial conditions in MPI-ESM. Hatched areas mark locations where the changes in frequency are out of range based on the empirical return periods provided by the sample size. (e–l) Local return levels of warm and cold extremes at four selected locations (marked as dots on the maps), representing the central Arctic (90°N, 0°E), northern Barents Sea (79°N, 50°E), North Atlantic (70°N, 0°E), and Siberia (73°N, 98°E) for different GWLs in MPI-ESM. The shading shows the uncertainty range of the return levels, estimated as the 90% confidence intervals based on bootstrap-resampling with replacement with 1,000 repetitions.

warming. This shows that sea-ice loss and subsequent Atlantification practically prevent the extreme cold that occurred under pre-industrial conditions.

Large (small) changes in the intensity of extreme temperatures go along with large (small) changes in frequency in most of the Arctic, but not everywhere (Figures 7b and 7d). The flatter the return level curve, the larger the changes in frequency for the same intensity change. In the North Atlantic (Figures 7g and 7k), the flat return level curves for both warm and cold extremes cause strong frequency changes of extreme events despite low changes in intensity, particularly in winter. For both warm and cold extremes, there are parts of the Arctic Ocean, especially the Barents Sea and North Atlantic sector, where the return levels at pre-industrial levels and 2°C GWL do not overlap. Consequently, frequency changes in these areas, hatched in Figures 7b and 7d, cannot be quantified. In practice, this means that these areas no longer experience temperatures that constituted a cold extreme at pre-

industrial levels. At the same time, they experience temperatures that constituted a warm extreme at pre-industrial levels every year, which can therefore no longer be considered extreme in a new Arctic climate.

6. Conclusions

Using five CMIP6 large ensembles, we assessed local, daily SAT in the Arctic under global warming, synthesizing changes in mean temperature, variability, seasonality, and extremes. As discussed above, the projected changes may be subject to model biases (Section 2.1) and, in part, depend on the pathway of global warming (Section 3). Nevertheless, the models paint a consistent picture of the changes in Arctic temperatures with global warming, which can be summarized as follows:

- The distribution of daily Arctic SAT changes considerably with global warming. Based on the Arctic-mean SAT, at 1.5 and 2°C of global warming, most of the days (84% [61%…95%] and 97% [93%…100%], respectively) will be warmer than extremely warm days at pre-industrial levels at the same time of year. At 3°C of global warming, virtually all days will be hotter than the extreme warm days at pre-industrial levels. The distinguishability of temperature distributions varies with season and region and is smaller on the local than on the pan-Arctic scale.
- Changes in the distribution primarily result from the shifting mean temperature. Annual Arctic-mean SAT increases 2.7 [2.3…3.1] times faster than the global average. This Arctic amplification underlies a strong seasonality, with seasonal mean warming being highest in winter (4.0 [3.6…4.6] times more than global warming) and lowest in summer (1.3 [0.9…1.7] times more than global warming).
- The variability of daily Arctic SAT decreases with global warming in all seasons except summer. Over the entire year, the variability of daily Arctic SAT decreases by 0.5 [0.4…0.6]°C (corresponding to about 8.5% of its pre-industrial value) per degree of global warming in the Arctic average. Temperature variability decreases most in autumn, associated with extensive sea-ice loss. In summer, the temperature variability stays approximately constant in the Arctic average.
- Due to the seasonality of Arctic warming, the amplitude of the seasonal cycle of Arctic SAT reduces by 2.1 [1.4…2.8]°C per degree of global warming, and the maxima and minima are reached some days later in the year. The shift in the day of maximum SAT is locally refined to areas of summer sea-ice loss, while the day of minimum SAT shifts more uniformly across the Arctic.
- The hottest days in the Arctic warm slightly more than the global average, whereas the coldest days warm 4–5 times more. For example, at 2°C of global warming, a 10-year warm extreme event is 2.5 [2.2…3.1]°C warmer, and a 10-year cold extreme event is 9.0 [7.6…10.0]°C warmer than under pre-industrial conditions in the Arctic average. While the intensity of extreme temperatures changes about linearly with global warming, the frequency changes almost exponentially, leading to substantial frequency changes. In particular, cold extreme events that occurred every few years in the pre-industrial Arctic will be virtually non-existent already at 1.5 or 2°C global warming.
- The local temperature changes vary regionally across the Arctic. Changes in every aspect of the local SAT distribution (mean warming, variability, seasonality, and extremes) are particularly large in areas of sea-ice loss. The region experiencing the most drastic temperature changes is the northern Barents Sea, undergoing an "Atlantification."

In summary, this study illustrates the transition to a new Arctic climate state with daily temperatures that significantly differ from pre-industrial levels. The amplified response of Arctic temperatures to anthropogenic greenhouse gas emissions underscores the importance of limiting global warming by every tenth of a degree to mitigate the severe impacts of Arctic warming on human and natural systems within and outside the region. At the same time, the projected reduction in temperature variability and extremely cold temperatures may ease the adaption to a warmer Arctic climate for some species.

Data Availability Statement

All data used for this study are publicly available. The CMIP6 data can be accessed from the Earth System Grid Federation (ESGF): https://esgf-data.dkrz.de/search/cmip6-dkrz/.

Acknowledgments
We thank Mika Rantanen and one anonymous reviewer for their constructive feedback. C.G., D.N., and J.B. acknowledge funding from the Deutsche Forschungsgemeinschaft under Germany's Excellence Strategy (EXC 2037; CLICCS—Climate, Climatic Change, and Society; project no. 390683824). This study is a contribution to the Cluster of Excellence "CLICCS—Climate, Climatic Change, and Society", contribution to the Center for Earth System Research and Sustainability (CEN) of Universität Hamburg. The data analysis for this study was performed with computing resources from the German Climate Computing Center (Deutsches Klimarechenzentrum, DKRZ). We acknowledge the World Climate Research Programme, which, through its Working Group on Coupled Modeling, coordinated and promoted CMIP6. We thank the climate modeling groups for producing and making available their model output, the Earth System Grid Federation (ESGF) for archiving the data and providing access, and the multiple funding agencies who support CMIP6 and ESGF. We acknowledge financial support from the Open Access Publication Fund of Universität Hamburg. Open Access funding enabled and organized by Projekt DEAL.

References

Alley, R. B., Marotzke, J., Nordhaus, W. D., Overpeck, J. T., Peteet, D. M., Pietke, R. A., et al. (2003). Abrupt climate change. *Science*, *299*(5615), 2005–2010. https://doi.org/10.1126/science.1081056

AMAP. (2021). Summary for policy-makers. In *Arctic climate change update 2021: Key trends and impacts* (pp. 1–16). Arctic Monitoring and Assessment Programme (AMAP).

Armstrong McKay, D. I., Staal, A., Abrams, J. F., Winkelmann, R., Sakschewski, B., Loriani, S., et al. (2022). Exceeding 1.5°C global warming could trigger multiple climate tipping points. *Science*, *377*(6611), eabn7950. https://doi.org/10.1126/science.abn7950

Bathiany, S., Dakos, V., Scheffer, M., & Lenton, T. M. (2018). Climate models predict increasing temperature variability in poor countries. *Science Advances*, *4*(5). https://doi.org/10.1126/sciadv.aar5809

Bintanja, R., & Van Der Linden, E. C. (2013). The changing seasonal climate in the Arctic. *Scientific Reports*, *3*(1), 1–8. https://doi.org/10.1038/srep01556

Blackport, R., Fyfe, J. C., & Screen, J. A. (2021). Decreasing subseasonal temperature variability in the northern extratropics attributed to human influence. *Nature Geoscience*, *14*(10), 719–723. https://doi.org/10.1038/S41561-021-00826-W

Boeke, R. C., Taylor, P. C., & Sejas, S. A. (2021). On the nature of the Arctic's positive lapse-rate feedback. *Geophysical Research Letters*, *48*(1), e2020GL091109. https://doi.org/10.1029/2020GL091109

Borodina, A., Fischer, E. M., & Knutti, R. (2017). Emergent constraints in climate projections: A case study of changes in high-latitude temperature variability. *Journal of Climate*, *30*(10), 3655–3670. https://doi.org/10.1175/JCLI-D-16-0662.1

Cai, Z., You, Q., Wu, F., Chen, H. W., Chen, D., & Cohen, J. (2021). Arctic warming revealed by multiple CMIP6 models: Evaluation of historical simulations and quantification of future projection uncertainties. *Journal of Climate*, *34*(12), 4871–4892. https://doi.org/10.1175/JCLI-D-20-0791.1

Chen, J., Dai, A., & Zhang, Y. (2019). Projected changes in daily variability and seasonal cycle of near-surface air temperature over the globe during the twenty-first century. *Journal of Climate*, *32*(24), 8537–8561. https://doi.org/10.1175/JCLI-D-19-0438.1

Chung, E. S., Ha, K. J., Timmermann, A., Stuecker, M. F., Bodai, T., & Lee, S. K. (2021). Cold-season Arctic amplification driven by Arctic Ocean-mediated seasonal energy transfer. *Earth's Future*, *9*(2), e2020EF001898. https://doi.org/10.1029/2020EF001898

Chylek, P., Folland, C., Klett, J. D., Wang, M., Hengartner, N., Lesins, G., & Dubey, M. K. (2022). Annual mean Arctic amplification 1970–2020: Observed and simulated by CMIP6 climate models. *Geophysical Research Letters*, *49*(13), e2022GL099371. https://doi.org/10.1029/2022GL099371

Collow, T. W., Wang, W., & Kumar, A. (2019). Reduction in northern midlatitude 2-m temperature variability due to Arctic sea ice loss. *Journal of Climate*, *32*(16), 5021–5035. https://doi.org/10.1175/JCLI-D-18-0692.1

Dai, A., & Deng, J. (2021). Arctic amplification weakens the variability of daily temperatures over northern middle-high latitudes. *Journal of Climate*, *34*(7), 2591–2609. https://doi.org/10.1175/JCLI-D-20-0514.1

Dai, A., Luo, D., Song, M., & Liu, J. (2019). Arctic amplification is caused by sea-ice loss under increasing CO_2. *Nature Communications*, *10*(1), 1–13. https://doi.org/10.1038/s41467-018-07954-9

Davy, R., & Outten, S. (2020). The Arctic surface climate in CMIP6: Status and developments since CMIP5. *Journal of Climate*, *33*(18), 8047–8068. https://doi.org/10.1175/JCLI-D-19-0990.1

Deser, C., Lehner, F., Rodgers, K. B., Ault, T., Delworth, T. L., DiNezio, P. N., et al. (2020). Insights from Earth system model initial-condition large ensembles and future prospects. *Nature Climate Change*, *10*(4), 277–286. https://doi.org/10.1038/s41558-020-0731-2

Dobricic, S., Russo, S., Pozzoli, L., Wilson, J., & Vignati, E. (2020). Increasing occurrence of heat waves in the terrestrial Arctic. *Environmental Research Letters*, *15*(2), 024022. https://doi.org/10.1088/1748-9326/ab6398

Duarte, C. M., Lenton, T. M., Wadhams, P., & Wassmann, P. (2012). Abrupt climate change in the Arctic. *Nature Climate Change*, *2*(2), 60–62. https://doi.org/10.1038/nclimate1386

Dwyer, J. G., Biasutti, M., & Sobel, A. H. (2012). Projected changes in the seasonal cycle of surface temperature. *Journal of Climate*, *25*(18), 6359–6374. https://doi.org/10.1175/JCLI-D-11-00741.1

England, M. R., Eisenman, I., Lutsko, N. J., & Wagner, T. J. (2021). The recent emergence of Arctic amplification. *Geophysical Research Letters*, *48*(15), e2021GL094086. https://doi.org/10.1029/2021GL094086

Eyring, V., Bony, S., Meehl, G. A., Senior, C. A., Stevens, B., Stouffer, R. J., & Taylor, K. E. (2016). Overview of the Coupled Model Intercomparison Project Phase 6 (CMIP6) experimental design and organization. *Geoscientific Model Development*, *9*(5), 1937–1958. https://doi.org/10.5194/gmd-9-1937-2016

Feldl, N., Po-Chedley, S., Singh, H. K., Hay, S., & Kushner, P. J. (2020). Sea ice and atmospheric circulation shape the high-latitude lapse rate feedback. *Npj Climate and Atmospheric Science*, *3*(1), 1–9. https://doi.org/10.1038/s41612-020-00146-7

Fischer, E. M., & Knutti, R. (2015). Anthropogenic contribution to global occurrence of heavy-precipitation and high-temperature extremes. *Nature Climate Change*, *5*(6), 560–564. https://doi.org/10.1038/nclimate2617

Graham, R. M., Cohen, L., Petty, A. A., Boisvert, L. N., Rinke, A., Hudson, S. R., et al. (2017). Increasing frequency and duration of Arctic winter warming events. *Geophysical Research Letters*, *44*(13), 6974–6983. https://doi.org/10.1002/2017GL073395

Hahn, L. C., Armour, K. C., Battisti, D. S., Eisenman, I., & Bitz, C. M. (2022). Seasonality in Arctic warming driven by sea ice effective heat capacity. *Journal of Climate*, *35*(5), 1629–1642. https://doi.org/10.1175/JCLI-D-21-0626.1

Hingray, B., & Säid, M. (2014). Partitioning internal variability and model uncertainty components in a multimember multimodel ensemble of climate projections. *Journal of Climate*, *27*(17), 6779–6798. https://doi.org/10.1175/JCLI-D-13-00629.1

Holland, M. M., & Landrum, L. (2021). The emergence and transient nature of Arctic amplification in coupled climate models. *Frontiers in Earth Science*, *9*, 764. https://doi.org/10.3389/feart.2021.719024

Holmes, C. R., Woollings, T., Hawkins, E., & de Vries, H. (2016). Robust future changes in temperature variability under greenhouse gas forcing and the relationship with thermal advection. *Journal of Climate*, *29*(6), 2221–2236. https://doi.org/10.1175/JCLI-D-14-00735.1

Huntingford, C., Jones, P. D., Livina, V. N., Lenton, T. M., & Cox, P. M. (2013). No increase in global temperature variability despite changing regional patterns. *Nature*, *500*(7462), 327–330. https://doi.org/10.1038/NATURE12310

Ingvaldsen, R. B., Assmann, K. M., Primicerio, R., Fossheim, M., Polyakov, I. V., & Dolgov, A. V. (2021). Physical manifestations and ecological implications of Arctic Atlantification. *Nature Reviews Earth & Environment*, *2*(12), 874–889. https://doi.org/10.1038/s43017-021-00228-x

IPCC. (2021). Summary for policymakers. In V. Masson-Delmotte, P. Zhai, A. Pirani, S. L. Connors, C. Péan, S. Berger, et al. (Eds.), *Climate change 2021: The physical science basis. Contribution of working group I to the sixth assessment report of the intergovernmental panel on climate change* (pp. 3–32). Cambridge University Press. https://doi.org/10.1017/9781009157896.001

Isaksen, K., Nordli, Ø., Ivanov, B., Køltzow, M. A. Ø., Aaboe, S., Gjelten, H. M., et al. (2022). Exceptional warming over the Barents area. *Scientific Reports*, *12*(1), 1–18. https://doi.org/10.1038/s41598-022-13568-5

James, R., Washington, R., Schleussner, C.-F., Rogelj, J., & Conway, D. (2017). Characterizing half-a-degree difference: A review of methods for identifying regional climate responses to global warming targets. *Wiley Interdisciplinary Reviews: Climate Change*, *8*(2), e457. https://doi.org/10.1002/WCC.457

Jansen, E., Christensen, J. H., Dokken, T., Nisancioglu, K. H., Vinther, B. M., Capron, E., et al. (2020). Past perspectives on the present era of abrupt Arctic climate change. *Nature Climate Change*, *10*(8), 714–721. https://doi.org/10.1038/s41558-020-0860-7

Jeffries, M. O., Overland, J. E., & Perovich, D. K. (2013). The Arctic shifts to a new normal. *Physics Today*, *66*(10), 35–40. https://doi.org/10.1063/PT.3.2147

Kharin, V. V., Flato, G. M., Zhang, X., Gillett, N. P., Zwiers, F., & Anderson, K. J. (2018). Risks from climate extremes change differently from 1.5°C to 2.0°C depending on rarity. *Earth's Future*, *6*(5), 704–715. https://doi.org/10.1002/2018EF000813

King, A. D., Borowiak, A. R., Brown, J. R., Frame, D. J., Harrington, L. J., Min, S.-K., et al. (2021). Transient and quasi-equilibrium climate states at 1.5°C and 2°C global warming. *Earth's Future*, *9*(11), e2021EF002274. https://doi.org/10.1029/2021EF002274

King, A. D., Lane, T. P., Henley, B. J., & Brown, J. R. (2020). Global and regional impacts differ between transient and equilibrium warmer worlds. *Nature Climate Change*, *10*(1), 42–47. https://doi.org/10.1038/s41558-019-0658-7

Landrum, L., & Holland, M. M. (2020). Extremes become routine in an emerging new Arctic. *Nature Climate Change*, *10*(12), 1108–1115. https://doi.org/10.1038/s41558-020-0892-z

Liang, Y. C., Polvani, L. M., & Mitevski, I. (2022). Arctic amplification, and its seasonal migration, over a wide range of abrupt CO_2 forcing. *Npj Climate and Atmospheric Science*, *5*(1), 1–9. https://doi.org/10.1038/s41612-022-00228-8

Lind, S., Ingvaldsen, R. B., & Furevik, T. (2018). Arctic warming hotspot in the northern Barents Sea linked to declining sea-ice import. *Nature Climate Change*, *8*(7), 634–639. https://doi.org/10.1038/s41558-018-0205-y

Mann, M. E., & Park, J. (1996). Greenhouse warming and changes in the seasonal cycle of temperature: Model versus observations. *Geophysical Research Letters*, *23*(10), 1111–1114. https://doi.org/10.1029/96GL01066

Moore, G. W. K. (2016). The December 2015 North Pole warming event and the increasing occurrence of such events. *Scientific Reports*, *6*(1), 1–11. https://doi.org/10.1038/srep39084

Olonscheck, D., & Notz, D. (2017). Consistently estimating internal climate variability from climate model simulations. *Journal of Climate*, *30*(23), 9555–9573. https://doi.org/10.1175/JCLI-D-16-0428.1

Olonscheck, D., Schurer, A. P., Lücke, L., & Hegerl, G. C. (2021). Large-scale emergence of regional changes in year-to-year temperature variability by the end of the 21st century. *Nature Communications*, *12*(1), 1–10. https://doi.org/10.1038/s41467-021-27515-x

Olonscheck, D., Suarez-Gutierrez, L., Milinski, S., Beobide-Arsuaga, G., Baehr, J., Fröb, F., et al. (2023). The new Max Planck Institute grand ensemble with CMIP6 forcing and high-frequency model output. *Journal of Advances in Modeling Earth Systems*, *15*(10), e2023MS003790. https://doi.org/10.1029/2023MS003790

Ono, J., Watanabe, M., Komuro, Y., Tatebe, H., & Abe, M. (2022). Enhanced Arctic warming amplification revealed in a low-emission scenario. *Communications Earth & Environment*, *3*(1), 1–9. https://doi.org/10.1038/s43247-022-00354-4

Pithan, F., & Mauritsen, T. (2014). Arctic amplification dominated by temperature feedbacks in contemporary climate models. *Nature Geoscience*, *7*(3), 181–184. https://doi.org/10.1038/ngeo2071

Polyakov, I. V., Ballinger, T. J., Lader, R., & Zhang, X. (2024). Modulated trends in Arctic surface air temperature extremes as a fingerprint of climate change. *Journal of Climate*, *37*(8), 2381–2404. https://doi.org/10.1175/JCLI-D-23-0266.1

Polyakov, I. V., Pnyushkov, A. V., Alkire, M. B., Ashik, I. M., Baumann, T. M., Carmack, E. C., et al. (2017). Greater role for Atlantic inflows on sea-ice loss in the Eurasian Basin of the Arctic Ocean. *Science*, *356*(6335), 285–291. https://doi.org/10.1126/SCIENCE.AAI8204

Previdi, M., Smith, K. L., & Polvani, L. M. (2021). Arctic amplification of climate change: A review of underlying mechanisms. *Environmental Research Letters*, *16*(9), 093003. https://doi.org/10.1088/1748-9326/AC1C29

Rantanen, M., Karpechko, A. Y., Lipponen, A., Nordling, K., Hyvärinen, O., Ruosteenoja, K., et al. (2022). The Arctic has warmed nearly four times faster than the globe since 1979. *Communications Earth & Environment*, *3*(1), 1–10. https://doi.org/10.1038/s43247-022-00498-3

Schneider, T., Bischoff, T., & Płotka, H. (2015). Physics of changes in synoptic midlatitude temperature variability. *Journal of Climate*, *28*(6), 2312–2331. https://doi.org/10.1175/JCLI-D-14-00632.1

Screen, J. A. (2014). Arctic amplification decreases temperature variance in northern mid- to high-latitudes. *Nature Climate Change*, *4*(7), 577–582. https://doi.org/10.1038/NCLIMATE2268

Screen, J. A., & Simmonds, I. (2010). The central role of diminishing sea ice in recent Arctic temperature amplification. *Nature*, *464*(7293), 1334–1337. https://doi.org/10.1038/nature09051

Seneviratne, S., Donat, M. G., Pitman, A. J., Knutti, R., & Wilby, R. L. (2016). Allowable CO_2 emissions based on regional and impact-related climate targets. *Nature*, *529*(7587), 477–483. https://doi.org/10.1038/nature16542

Seneviratne, S., Zhang, X., Adnan, M., Badi, W., Dereczynski, C., Luca, A. D., et al. (2021). Weather and climate extreme events in a changing climate. In V. Masson-Delmotte, et al. (Eds.), *Climate change 2021: The physical science basis. Contribution of working group I to the sixth assessment report of the intergovernmental panel on climate change* (pp. 1513–1766). https://doi.org/10.1017/9781009157896.013

Serreze, M. C., & Barry, R. G. (2011). Processes and impacts of Arctic amplification: A research synthesis. *Global and Planetary Change*, *77*(1–2), 85–96. https://doi.org/10.1016/j.gloplacha.2011.03.004

Stine, A. R., Huybers, P., & Fung, I. Y. (2009). Changes in the phase of the annual cycle of surface temperature. *Nature*, *457*(7228), 435–440. https://doi.org/10.1038/nature07675

Stouffer, R. J., & Wetherald, R. T. (2007). Changes of variability in response to increasing greenhouse gases. Part I: Temperature. *Journal of Climate*, *20*(21), 5455–5467. https://doi.org/10.1175/2007JCLI1384.1

Swart, N. C., Cole, J. N., Kharin, V. V., Lazare, M., Scinocca, J. F., Gillett, N. P., et al. (2019). The Canadian Earth System Model version 5 (CanESM5.0.3). *Geoscientific Model Development*, *12*(11), 4823–4873. https://doi.org/10.5194/GMD-12-4823-2019

Sweeney, A. J., Fu, Q., Po-Chedley, S., Wang, H., & Wang, M. (2023). Internal variability increased Arctic amplification during 1980–2022. *Geophysical Research Letters*, *50*(24), e2023GL106060. https://doi.org/10.1029/2023GL106060

Tamarin-Brodsky, T., Hodges, K., Hoskins, B. J., & Shepherd, T. G. (2020). Changes in Northern Hemisphere temperature variability shaped by regional warming patterns. *Nature Geoscience*, *13*(6), 414–421. https://doi.org/10.1038/s41561-020-0576-3

Tatebe, H., Ogura, T., Nitta, T., Komuro, Y., Ogochi, K., Takemura, T., et al. (2019). Description and basic evaluation of simulated mean state, internal variability, and climate sensitivity in MIROC6. *Geoscientific Model Development*, *12*(7), 2727–2765. https://doi.org/10.5194/GMD-12-2727-2019

Thomson, D. J. (1995). The seasons, global temperature, and precession. *Science*, *268*(5207), 59–68. https://doi.org/10.1126/SCIENCE.268.5207.59

Tian, T., Yang, S., Høyer, J. L., Nielsen-Englyst, P., & Singha, S. (2024). Cooler Arctic surface temperatures simulated by climate models are closer to satellite-based data than the ERA5 reanalysis. *Communications Earth & Environment*, *5*(1), 1–6. https://doi.org/10.1038/s43247-024-01276-z

Walsh, J. E., Ballinger, T. J., Euskirchen, E. S., Hanna, E., Mård, J., Overland, J. E., et al. (2020). Extreme weather and climate events in northern areas: A review. *Earth-Science Reviews*, *209*, 103324. https://doi.org/10.1016/J.EARSCIREV.2020.103324

Wartenburger, R., Hirschi, M., Donat, M. G., Greve, P., Pitman, A. J., & Seneviratne, S. I. (2017). Changes in regional climate extremes as a function of global mean temperature: An interactive plotting framework. *Geoscientific Model Development*, *10*(9), 3609–3634. https://doi.org/10.5194/GMD-10-3609-2017

Wendisch, M., Brückner, M., Crewell, S., Ehrlich, A., Notholt, J., Lüpkes, C., et al. (2023). Atmospheric and surface processes, and feedback mechanisms determining Arctic amplification: A review of first results and prospects of the (AC)3 project. *Bulletin of the American Meteorological Society*, *104*(1), E208–E242. https://doi.org/10.1175/BAMS-D-21-0218.1

Wyser, K., Koenigk, T., Fladrich, U., Fuentes-Franco, R., Karami, M. P., & Kruschke, T. (2021). The SMHI large ensemble (SMHI-LENS) with EC-Earth3.3.1. *Geoscientific Model Development*, *14*(7), 4781–4796. https://doi.org/10.5194/GMD-14-4781-2021

Ylhäisi, J. S., & Räisänen, J. (2014). Twenty-first century changes in daily temperature variability in CMIP3 climate models. *International Journal of Climatology*, *34*(5), 1414–1428. https://doi.org/10.1002/JOC.3773

Zhou, W., Leung, L. R., & Lu, J. (2024). Steady threefold Arctic amplification of externally forced warming masked by natural variability. *Nature Geoscience*, *17*(6), 508–515. https://doi.org/10.1038/s41561-024-01441-1

Ziehn, T., Chamberlain, M. A., Law, R. M., Lenton, A., Bodman, R. W., Dix, M., et al. (2020). The Australian Earth system model: ACCESS-ESM1.5. *Journal of Southern Hemisphere Earth Systems Science*, *70*(1), 193–214. https://doi.org/10.1071/ES19035